Jeans instability in partially ionized self-gravitating dusty plasmas

F. Verheest,[1] P. K. Shukla,[2,*] G. Jacobs,[1] and V. V. Yaroshenko[3]
[1]*Sterrenkundig Observatorium, Universiteit Gent, Krijgslaan 281, B-9000, Gent, Belgium*
[2]*Fakultät für Physik und Astronomie, Ruhr-Universität Bochum, D-44780 Bochum, Germany*
[3]*Max-Planck Institute for Extraterrestrial Physics, Postfach 1312, D-85741 Garching, Germany*
(Received 3 February 2003; published 11 August 2003)

By employing the Boltzmann distributions for electrons and ions and by retaining the full dynamics of charged dust and neutral fluids, we derive a dispersion law for coupled dust-acoustic and neutral sound waves in partially ionized self-gravitating dusty plasmas. This dispersion law exhibits new classes of Jeans instability in both collisionless and highly collisional regimes. The result should help understand the origin of molecular cloud collapse in interstellar space.

DOI: 10.1103/PhysRevE.68.027402 PACS number(s): 52.27.Lw, 52.35.Fp, 02.30.Yy

I. INTRODUCTION AND MODEL

Partially ionized self-gravitating dusty plasmas are composed of electrons, ions, charged dust grains, and neutrals. They are frequently found in interstellar molecular clouds, supernovae, stars and planetary nebulas, and cometary tails and comas, where micron-sized dust grains, surrounded by partially ionized media and radiative environments, can become highly charged. In astrophysical systems containing massive charged dust grains, long-range gravitational and electromagnetic forces could be of equal importance in studying wave phenomena and instabilities [1–8].

Previous studies [5–7] have shown that in dusty plasmas with stationary neutrals the criteria for the Jeans instability [9] involve the dust-acoustic velocity [10] in an unmagnetized self-gravitating plasma. However, in astrophysical objects [11–15] the mass densities of neutrals and charged dust typically are comparable. Thus, it is of great interest to study the Jeans instability in a self-gravitating partially ionized dusty plasma, keeping the full dynamics of neutrals and charged dust grains on an equal footing. On the relevant Jeans collapse scales, the friction between the two heavy species is most important, since the lighter electrons and ions are almost perfectly Boltzmann distributed and carry little inertia, but do provide pressure.

The model we investigate is a collisional dusty plasma consisting of electrons, ions, and charged and neutral dust grains where collisions between the two dust species are the dominant ones, providing friction between the heavier components of the combined plasma. For electrostatic waves with phase speeds much smaller than the thermal speeds of the electrons and plasma ions, these can be treated as Boltzmann distributed:

$$n_\alpha = n_{\alpha 0} \exp\left(-\frac{q_\alpha \psi_E}{\kappa T_\alpha}\right) \qquad (\alpha = e, i). \tag{1}$$

To describe the dynamics of the charged and neutral dust particles we use the continuity equations

$$\frac{\partial n_\alpha}{\partial t} + \frac{\partial}{\partial x}(n_\alpha v_\alpha) = 0 \qquad (\alpha = d, n) \tag{2}$$

and the equations of motion

$$\frac{\partial v_d}{\partial t} + v_d \frac{\partial v_d}{\partial x} + \frac{q_d}{m_d}\frac{\partial \psi_E}{\partial x} + \frac{\partial \psi_G}{\partial x} + \frac{v_{Td}^2}{n_d}\frac{\partial n_d}{\partial x} + \nu_{dn}(v_d - v_n) = 0,$$

$$\frac{\partial v_n}{\partial t} + v_n \frac{\partial v_n}{\partial x} + \frac{\partial \psi_G}{\partial x} + \frac{v_{Tn}^2}{n_n}\frac{\partial n_n}{\partial x} + \nu_{nd}(v_n - v_d) = 0. \tag{3}$$

Different species have densities, fluid velocities, charge, and mass, respectively, denoted by n_α, v_α, q_α, and m_α. The species label α is e for electrons, i for ions, d for charged and n for neutral dust. Thermal velocities are $v_{T\alpha}$, while ν_{dn} and ν_{nd} are the collision frequencies between the charged and neutral dust, respectively, related through $m_n n_{n0} \nu_{nd} = m_d n_{d0} \nu_{dn}$. The electric potential ψ_E and the gravitational potential ψ_G obey the Poisson equations

$$\frac{\partial^2 \psi_E}{\partial x^2} = \frac{1}{\varepsilon_0}(n_e e - n_i e - n_d q_d),$$

$$\frac{\partial^2 \psi_G}{\partial x^2} = 4\pi G(m_d n_d + m_n n_n), \tag{4}$$

which close the set of basic equations.

II. DISPERSION LAW

Assuming perturbations proportional to $\exp[ikx - i\omega t]$, we obtain after linearizing Eqs. (1)–(4) the dispersion law

*Also at Department of Plasma Physics, Umeå University, S-90187 Umeå, Sweden.

$$[\omega(\omega+i\nu_{dn})-k^2v_{Td}^2-k^2c_{da}^2+\omega_{Jd}^2]\left[\omega\left(\omega+i\nu_{dn}\frac{\omega_{Jd}^2}{\omega_{Jn}^2}\right)-k^2v_{Tn}^2+\omega_{Jn}^2\right]=\left[\omega_{Jd}\omega_{Jn}-i\omega\nu_{dn}\frac{\omega_{Jd}}{\omega_{Jn}}\right]^2. \quad (5)$$

Here $\lambda_{D\alpha}^2=\varepsilon_0\kappa T_\alpha/n_{\alpha0}q_\alpha^2$, $\omega_{p\alpha}^2=n_{\alpha0}q_\alpha^2/\varepsilon_0 m_\alpha$, and $\omega_{J\alpha}^2=4\pi G n_{\alpha0}m_\alpha$ are, respectively, the squares of the Debye length, the plasma, and the Jeans frequencies of species α. We have also introduced the global plasma Debye length λ_D through $\lambda_D^{-2}=\lambda_{De}^{-2}+\lambda_{Di}^{-2}$ and the dust-acoustic velocity $c_{da}=\lambda_D\omega_{pd}$. The form of Eq. (5) clearly shows that the dust-acoustic and neutral sound waves are coupled, due to friction, in a complicated fashion. Analysis of the dispersion law will exhibit significant modifications of the Jeans instability in a partially ionized dusty plasma, the generic features of which will be confirmed by the rootlocus approach [16].

When substituting $\omega=i\Omega$ in dispersion law (5), we obtain a quartic equation with real coefficients, viz.,

$$\Omega^4+A\Omega^2+B+\frac{\nu_{dn}(\omega_{Jd}^2+\omega_{Jn}^2)}{\omega_{Jn}^2}\Omega[\Omega^2-C]=0, \quad (6)$$

where

$$A=k^2(c_{da}^2+v_{Td}^2+v_{Tn}^2)-\omega_{Jd}^2-\omega_{Jn}^2,$$

$$B=k^4(c_{da}^2+v_{Td}^2)v_{Tn}^2-k^2(c_{da}^2+v_{Td}^2)\omega_{Jn}^2-k^2v_{Tn}^2\omega_{Jd}^2,$$

$$C=\omega_{Jd}^2+\omega_{Jn}^2-k^2\frac{(c_{da}^2+v_{Td}^2)\omega_{Jd}^2+v_{Tn}^2\omega_{Jn}^2}{\omega_{Jd}^2+\omega_{Jn}^2}. \quad (7)$$

Since $\nu_{dn}/\omega_{Jn}^2=\nu_{nd}/\omega_{Jd}^2$, we could use either expression in Eq. (6), from which we also note that

$$\Omega^4+A\Omega^2+B=0 \quad (8)$$

corresponds to the collisionless dispersion law. The discriminant of this biquadratic equation can be shown to be strictly positive, implying that both roots Ω^2, viz., r_1 and r_2, are real and different. The roots are numbered such that $r_1>r_2$, and the strict inequality is a consequence of our implicit ansatz, that both charged and neutral dust have nonzero densities. Otherwise, we revert to fully ionized dusty plasmas, dealt with before [5,6,8], or to plasmas without charged dust at all.

In the case of friction between light plasma ions and heavy charged dust (in the absence of neutrals) an easy separation between the roots was possible owing to the vastly different frequency domains [8]. Here, on the other hand, it is not *a priori* possible to tell whether r_1 refers primarily to the charged or to the neutral dust mode, as that will depend on their relative mass densities occurring in the Jeans frequencies.

Since $A=-(r_1+r_2)$, $B=r_1r_2$, and C can change sign, it is necessary to determine the critical k values where this occurs:

TABLE I. Classification for different wave number regions.

k		k_A		k_C		k_B	
A	$-$	0	+	+	+	+	+
B	$-$	$-$	$-$	$-$	$-$	0	+
C	+	+	+	0	$-$	$-$	$-$
Case	I		II		III		IV

$$k_A^2=\frac{\omega_{Jd}^2+\omega_{Jn}^2}{c_{da}^2+v_{Td}^2+v_{Tn}^2},$$

$$k_B^2=\frac{\omega_{Jd}^2}{c_{da}^2+v_{Td}^2}+\frac{\omega_{Jn}^2}{v_{Tn}^2},$$

$$k_C^2=\frac{(\omega_{Jd}^2+\omega_{Jn}^2)^2}{(c_{da}^2+v_{Td}^2)\omega_{Jd}^2+v_{Tn}^2\omega_{Jn}^2}. \quad (9)$$

It is clear that the dust-neutral collisions exert a different influence in wave number regions separated by the critical values k_A, k_B, and k_C, ordered such that $k_A<k_C<k_B$. Consequently, there are four regions in parameter space, as shown in Table I. The behavior of A and B is of importance for the collisionless part of Eq. (6), whereas C comes in when the collision frequency is nonzero.

Before going on, however, we make some additional remarks concerning the collisionless dispersion law (8), which has one stable and one unstable root in Ω^2 (or in ω^2) for $B<0$, viz. in regions I, II, and III. In region IV, where $A>0$ and $B>0$, both roots r_1 and r_2 are negative, which means two positive roots for ω^2, and hence there is no instability. Furthermore, if we identify $x=k^2$ and $y=\Omega^2$, it can readily be ascertained that Eq. (8) corresponds to a hyperbola. At $x=k^2=0$, the corresponding values for $y=\Omega^2$ are 0 and $\omega_{Jd}^2+\omega_{Jn}^2$. The tangent T in $(0,\omega_{Jd}^2+\omega_{Jn}^2)$ to this hyperbola is given by

$$\frac{k^2}{k_C^2}+\frac{\Omega^2}{\omega_{Jd}^2+\omega_{Jn}^2}=1, \quad (10)$$

and not only connects the points $(0,\omega_{Jd}^2+\omega_{Jn}^2)$ and $(k_C^2,0)$ but also represents the relation $\Omega^2=C$. Hence, r_1 is the branch of the hyperbola lying above T and going through $k^2=0$, $\Omega^2=\omega_{Jd}^2+\omega_{Jn}^2$. Then the lower branch through $k^2=\Omega^2=0$ is r_2, lying completely below T. Both are shown in Fig. 1. For all real k^2 we find that $r_2\leqslant 0$, whereas $r_1>0$ for $0\leqslant k^2<k_B^2$ (corresponding to regions I, II, and III), and $r_1<0$ for $k^2>k_B^2$ (region IV). Thus, r_2 corresponds in ω^2 to a stable root, whereas r_1 is unstable (in ω^2) in $0\leqslant k^2<k_B^2$.

III. STABILITY AND INSTABILITY

We now rewrite Eq. (6) in the compact form

$$(\Omega^2-r_1)(\Omega^2-r_2)+\tilde{\nu}\Omega(\Omega^2-C)=0 \quad (11)$$

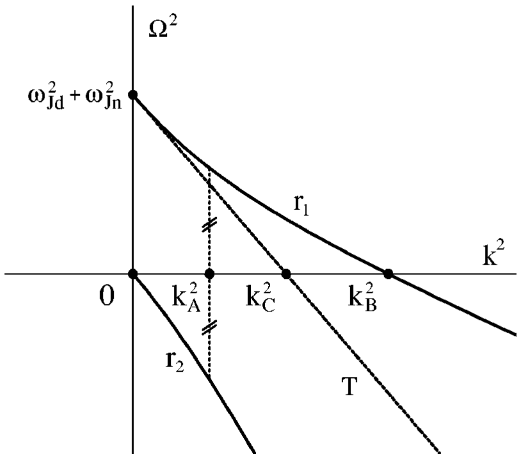

FIG. 1. Plot of the branches r_1 and r_2 of the hyperbola representing the collisionless dispersion law Eq. (8), whereas the tangent T is the plot of $\Omega^2=C$.

in terms of $\tilde{\nu}=\nu_{dn}(\omega_{Jd}^2+\omega_{Jn}^2)/\omega_{Jn}^2$, a normalized dust-neutral collision frequency. As Eq. (11) is of the form $D(\Omega)+\tilde{\nu}N(\Omega)=0$, where $D(\Omega)$ and $N(\Omega)$ are polynomials with real coefficients and $\tilde{\nu}$ is a real and positive parameter, it can be analyzed using the semianalytical rootlocus method [16]. Such a plot sketches the evolution of the roots of Eq. (11) in the complex frequency plane, as the normalized collision frequency $\tilde{\nu}$ increases from zero to infinity. Consequently, a rootlocus plot will start in the roots of the collisionless dispersion law (8), represented by crosses in the figures. On the other hand, the mathematical limit $\tilde{\nu}\rightarrow\infty$ corresponds to the trivial solutions $\Omega=0$ and $\Omega=\pm\sqrt{C}$. These represent the end points of the loci and are depicted by circles. Evidently, extremely large values of the collision frequency are not physically relevant, but are mathematically needed for the proper construction of the rootlocus plots. The rootloci plots have been computed in terms of Ω, but were afterwards rotated counterclockwise over 90°, in order to connect the horizontal axis with real values of ω so that the

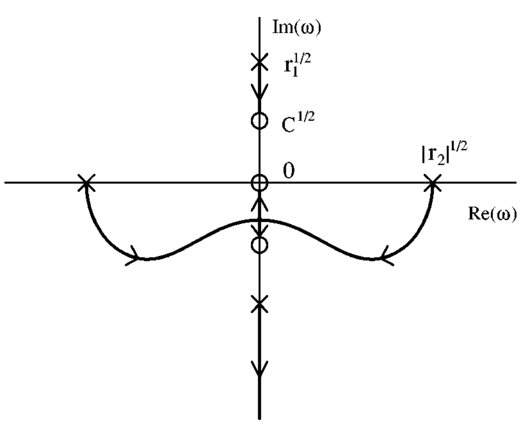

FIG. 2. Typical rootlocus plot for region II, with wave numbers $k_A<k<k_C$. The crosses and circles correspond to the poles and zeros, respectively, of $\Omega(\Omega^2-C)/(\Omega^2-r_1)(\Omega^2-r_2)$, whereas the arrows are directed towards increasing collision frequencies.

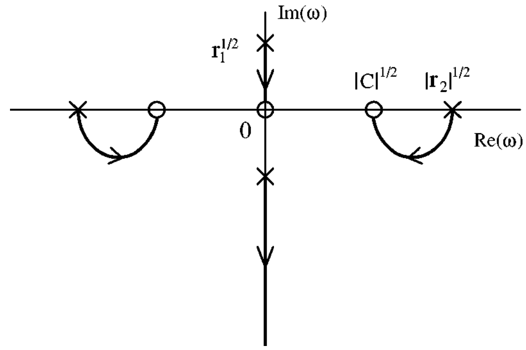

FIG. 3. Typical rootlocus plot corresponding to region III with wave numbers $k_C<k<k_B$.

figures can readily be interpreted. Examples will be given in Figs. 2 and 3, discussed in more detail below.

The general features of rootlocus plots [8,16] allow us to determine some of the important features of the figures effortlessly. For instance, the figures will be symmetrical with respect to the vertical axis. Moreover, intervals on the vertical axis that belong entirely to the plot can be immediately recognized for each of the wave number regions. In this manner, one can see that wave number region IV is stable, as we knew already, whereas the other regions remain unstable, regardless of the value of the collision frequency. Additionally, the evolution of the growth rate of the unstable mode is visualized for all regions. Lastly, the asymptotic behavior of the plots, i.e., for $\tilde{\nu}\rightarrow 0$ and $\tilde{\nu}\rightarrow\infty$ can be readily sketched for each wave number region.

Since the rootlocus plots starting from $\pm|r_2|^{1/2}$ leave the real axis in a perpendicular direction downward, this indicates that Re ω will initially show little change compared to its value in the absence of charged-neutral collisions. However, there quickly occurs increasing damping. At larger collision frequencies, the real part of the wave frequency is also affected.

We also remark that Eq. (11) has no purely imaginary solutions (in Ω) for nonzero, finite values of the collision frequency, and thus a general form of the rootlocus plot can be obtained for each of the unstable wave number regions I, II, and III. For that we need to compare the absolute values of r_1, r_2, and C in the different regions, shown in Table II. The rootlocus plots can be constructed in analogy with our discussion of the influence of ion-dust collisions in a dusty plasma without neutrals [8].

To fix the ideas, rootlocus plots have been computed for $\omega_{Jd}\simeq\omega_{Jn}$ and $c_{da}\simeq 10\,v_{Tn}$, and Fig. 2 depicts the qualitative

TABLE II. Ordering in different regions.

Region	Ordering
I	$\lvert r_2\rvert<r_1$ and $0<C<r_1$
II	$0<C<r_1<\lvert r_2\rvert$
III	$\lvert C\rvert<\lvert r_2\rvert$ and $r_1<\lvert r_2\rvert$
IV	$\lvert r_1\rvert<\lvert C\rvert<\lvert r_2\rvert$

behavior of the evolution of the rootloci for region II. For region I, the rootlocus plot (not shown) has a similar behavior, but the ordering between r_1 and r_2 is reversed, and $r_1 \simeq C$, so that the growth rate of the unstable mode is hardly influenced. Going to higher wave numbers, viz., $k_C < k < k_B$ (region III), the qualitative form of the rootlocus plots changes and is depicted in Fig. 3. The rootlocus plots for the stable wave number region IV can have different forms but are not given here, since they relate to stable waves.

We conclude that for the unstable wave number regions, the growth rate of the unstable mode clearly diminishes for increasing collision frequencies, whereas the stable zero frequency mode becomes increasingly damped. The remaining stable frequency modes are damped while their real frequency reduces.

IV. CONCLUSIONS

In summary, we have presented an investigation of the Jeans instability in a self-gravitating dusty plasma, accounting for the charged and neutral dust fluid dynamics on an equal footing. We have obtained a dispersion law that exhibits the linear coupling between the dust-acoustic and neutral sound wave in a nontrivial fashion.

Consideration of the neutral fluid dynamics significantly affects the growth rate of the Jeans instability. As a powerful and generic alternative to a numerical evaluation of the dispersion to see the interplay between the Jeans modes in a dusty plasma and in a neutral fluid, we have used the rootlocus method to illustrate qualitatively how the real frequency and damping decrement of these Jeans modes change over the spectrum of collision frequencies. We have thus shown that the growth rate of the unstable zero frequency mode diminishes at increasing collision frequencies, whereas the stable counterpart becomes increasingly damped. On the other hand, the remaining stable frequency modes are damped while their real frequency is reduced. Charge-neutral friction thus makes the unstable mode grow slower but cannot stabilize it, while previously stable modes become damped.

In conclusion, the results of our investigations should be useful in understanding the collapse of molecular clouds in interstellar space, which are composed of electrons and ions, and of charged dust grains in the presence of a sizeable fraction of neutrals. For the self-gravitational aspects of this collapse it is the friction between the two heavy species that is most important. On the relevant collapse scales, the lighter electrons and ions carry little inertia and cannot contribute much to friction, but they do provide pressure.

ACKNOWLEDGMENTS

F.V. and G.J. thank the Fonds voor Wetenschappelijk Onderzoek (Vlaanderen) for a research grant. The work of P.K.S. was partially supported by the Deutsche Forschungsgemeinschaft through the Sonderforschungsbereich 591 and by the European Commission (Brussels) through Contract No. HPRN-CT-2000-00140. V.V.Y. acknowledges the support of the Alexander von Humboldt Foundation.

[1] P. Bliokh, V. Sinitsin, and V. Yaroshenko, *Dusty and Self-Gravitational Plasmas in Space* (Kluwer, Dordrecht, 1995).
[2] F. Verheest, *Waves in Dusty Space Plasmas* (Kluwer, Dordrecht, 2000).
[3] P.K. Shukla and A.A. Mamun, *Introduction to Dusty Plasma Physics* (IOP, Bristol, 2002).
[4] P.K. Shukla, *Dust Plasma Interaction in Space* (Nova Science, New York, 2002).
[5] K. Avinash and P.K. Shukla, Phys. Lett. A **189**, 470 (1994).
[6] B.P. Pandey, K. Avinash, and C.B. Dwivedi, Phys. Rev. E **49**, 5599 (1994).
[7] P.K. Shukla and F. Verheest, Astrophys. Space Sci. **262**, 157 (1999).
[8] G. Jacobs, V.V. Yaroshenko, and F. Verheest, Phys. Rev. E **66**, 026407 (2002).
[9] J.H. Jeans, *Astronomy and Cosmogony* (Cambridge University Press, Cambridge, 1929).
[10] N.N. Rao, P.K. Shukla, and M.Y. Yu, Planet. Space Sci. **38**, 543 (1990).
[11] E.G. Zweibel, Phys. Plasmas **6**, 1725 (1999).
[12] V. Krishan, *Astrophysical Plasmas and Fluids* (Kluwer, Dordrecht, 1999).
[13] H. Kamaya and R. Nishi, Astrophys. J. **543**, 257 (2000).
[14] T. Nakano, R. Nishi, and T. Umbayashi, Astrophys. J. **573**, 199 (2002).
[15] L.I. Rudakov, Phys. Scr. **T89**, 158 (2001).
[16] J. Willems, *Stability Theory of Dynamical Systems* (Nelson, London, 1970).